View metadata, citation and similar papers at core.ac.uk
brought to you by CORE
provided by TELKOMNIKA (Telecommunication Computing Electronics and Control)

TELKOMNIKA, Vol.15, No.3, September 2017, pp. 1003~1011
ISSN: 1693-6930, accredited **A** by DIKTI, Decree No: 58/DIKTI/Kep/2013
DOI: 10.12928/TELKOMNIKA.v15i3.5439

A Three-Phase Grid-Connected PV System Based on SAPF for Power Quality Improvement

Rachid Belaidi*[1], Ali Haddouche[2], Djamila Ghribi[3], M.Mghezzi Larafi[4]
[1,2]Electromechanical Engineering Laboratory, Badji Mokhtar University, BP 12, 23000, Annaba, Algeria
[1,3,4]Development Unit of Solar Equipments, UDES, EPST/ CDER, 42415, Tipaza, Algeria
*Corresponding author, e-mail: rachidbelaidi@yahoo.fr

Abstract

This paper proposes a combined system of three-phase four-wire shunt active power filter (SAPF), and photovoltaic generator (PVG), to solve the power quality problems such as harmonic currents, poor power factor, and unbalanced load. In addition, the proposed system can inject the issued energy from the PVG into the utility grid. To increase the efficiency of the PVG and extract the maximum photovoltaic (PV) power under variable atmospheric conditions, a maximum power point tracking (MPPT) technique based on perturb and observe (P&O) is implemented in the DC/DC boost converter. The effectiveness of the proposed PVG-SAPF (PVG and SAPF) based on the use of synchronous reference frame theory (SRF theory) under unbalanced nonlinear load. The proposed PVG-SAPF is validated through numerical simulations using Matlab/Simulink software. The simulation results show the effectiveness of the proposed PVG-SAPF.

Keywords*: power quality, shunt active power filter, SRF theory, PV system and MPPT*

Copyright © 2017 Universitas Ahmad Dahlan. All rights reserved.

1. Introduction

In the last decades, renewable energy sources have attracted much more attention due to the advantages such as less environmental impact and offer clean and abundant energy. Oday solar energy become one of the most famed energy sources. With the growth of command tools, solar energy is not limited to the generation of active power into the network, but it also participates in power quality improvement [1-6]. The traditional passive power filters was a famous solution for harmonics filtering [4, 7, 8]. However, in functional implementation, they attend many drawbacks such as limited compensation, big size, and resonance with the network impedances [4, 9].

New active power filters provide high filtering performances with more flexibility and reduced size. They have many functions such as harmonic mitigation, correction of power factor and balancing of the load [4, 9].

To take out the maximum power from the PVG, a lot of MPPT algorithms have been developed in the literature, the most used methods are “perturb and observe” (P&O) [13, 14]. [10-12] and incremental conductance techniques [13, 14].

This paper presents a simulation of a system composed of a three-phase four-wire SAPF, and PVG to improve the electrical power quality. The PVG-SAPF controller generates reference currents using SRF theory under unbalanced nonlinear load. the step-up converter is controlled using a P&O-based MPPT technique.

The remainder of the paper is organized as follows: the next section presents the modeling of the PV system, its I-V and P-V characteristics, MPPT and (P&O) technique. The third section presents the design and control of PVG-SAPF, The fourth section displays simulation results and discussion and the last section of this paper consists of a conclusion.

2. PV System

2.1. PV Model and Characteristics

A PV solar cell is a semiconductor material that converts solar irradiation into electric energy [15]. Many models of PV cell are presented in the literature, such as a single-diode [10], and two-diode model [16].

Received April 30, 2017; Revised August 1, 2017; Accepted August 15, 2017

The model used in this study is the two diodes model, where the shunt and series resistors are taking into consideration as shown in Figure 1. The model consists of a current source I_{ph} in parallel with two diodes, a series resistor R_S and a parallel resistor R_{Sh}.

Table.1 Technical Module Characteristics

Electrical characteristics	Symbols	Values
Maximum power (W) at STC	P_{mpp}	219.72
Maximum power voltage (V)	V_{mpp}	48.315
Maximum power current (A)	I_{mpp}	4.5475
Open circuit voltage (V)	V_{oc}	59.261
Short circuit current (A)	I_{sc}	5.0926

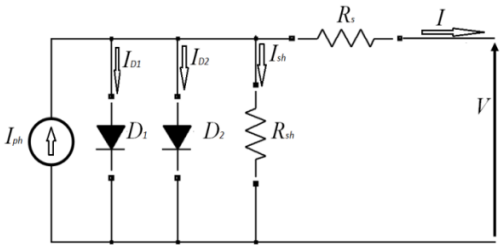

Figure 1. PV solar cell Model with two diodes

The following equation gives the exponential equation of the PV cell current and and the PV cell voltage:

$$I = I_{ph} - I_{s1}(e^{\frac{q(V+IR_s)}{n1KT}} - 1) - I_{s2}(e^{\frac{q(V+IR_s)}{n2KT}} - 1) - \frac{(V+IR_s)}{R_{sh}} \quad (1)$$

Where V and I represent the output voltage and current of the PV cell, I_{s1} and I_{s2} are diodes saturation currents; q is coulomb constant, K is Boltzman's constant, T is cell temperature (K); n_1 and n_2 are P-N junction ideality factor.

In this paper, the used module is CS5P-220M, the technical module characteristics are given in Table 1. The I-V and P-V PV module characteristics within STC conditions test are presented in Figure 2.

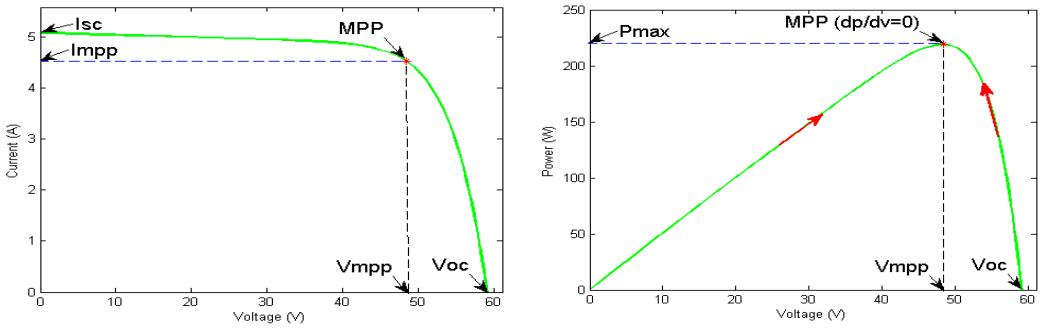

Figure 2. *I–V* and *P–V* PV module characteristics at STC.

Figure 3 shows the *I-V* and *P-V* characteristics of a PV module with different irradiations and at a constant temperature (T=25C°), while Figure 4 shows the *P-V* and *I-V* characteristics of a PV module with different temperature and at a constant irradiations (G=1000 W/m^2).

As shown in these figures, the PV power increases with the increasing of irradiance. Thus, the maximum power point (MPP) decreases with the decreases of irradiance. On the other hand, the PV power decreases with the increasing of temperature. Therefore, the MPP increases with the decrease of temperature.

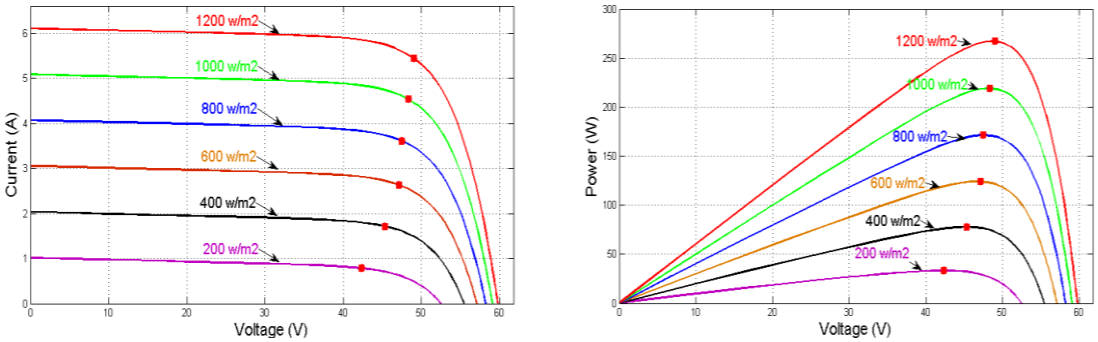

Figure 3. *I–V* and *P–V* characteristics of a PV module within various irradiations and at a constant temperature *T*= 25 C°

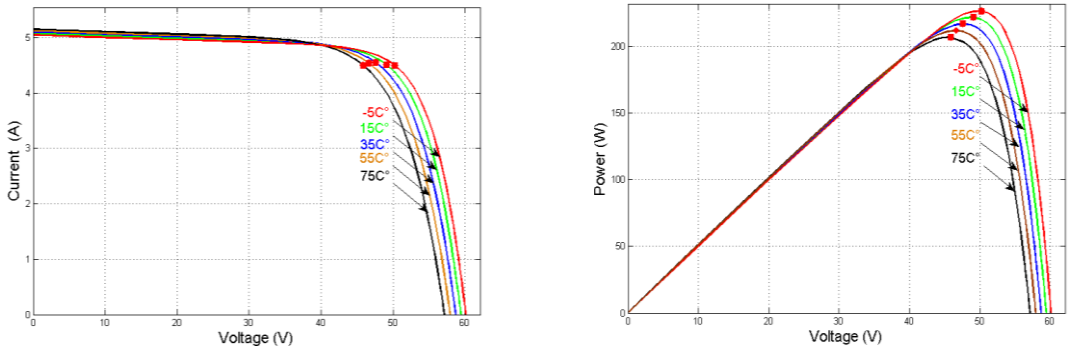

Figure 4. *I–V* and *P–V* characteristics of a PV module within various temperature and at a constant irradiation *G*=1000 W/m^2

2.2. Perturb and Observe (P&Q) MPPT Technique

Among the most used MPPT techniques in the literature is Perturb and Observe (P&O), because of its low cost, and simplicity [17]. The execution of this algorithm needs current and voltage sensors to find the output power, and provokes a perturbation on the duty cycle D. Each sampling period the duty cycle is updated as a power variation function. Figure 5 shows the flowchart of the P&O algorithm, while Figure 6 shows the Simulink block of P&O algorithm.

2.3. Step-up converter

The step-up converter is applied to connect the load and the PVG for optimum operation of the system. The step-up converter output voltage (V_{out}), the PVG voltage (V_{in}) and the duty cycle *D* are gives:

$$\frac{V_{out}}{V_{in}} = \frac{1}{1-D} \tag{2}$$

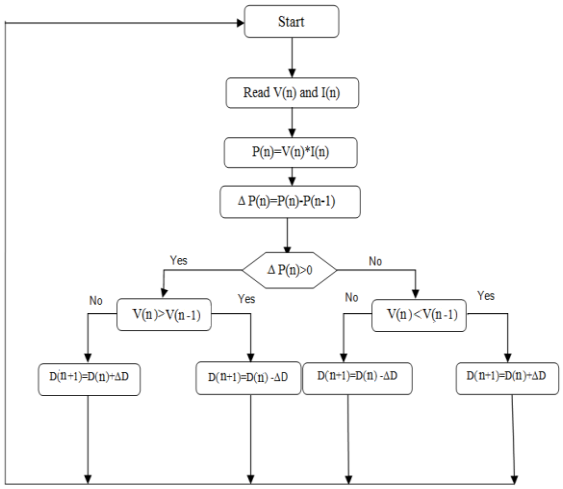

Figure 5. Flowchart of the P&O algorithm

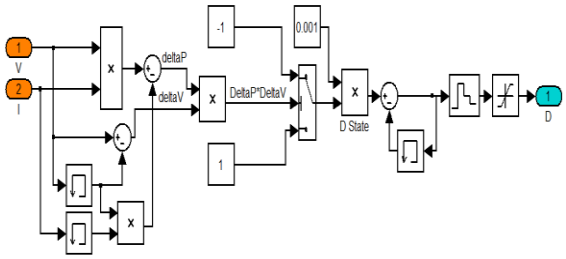

Figure 6. Simulink diagram of P&O algorithm

3. Shunt Active Power Filter Topology

The proposed system (PVG-SAPF) consists of a photovoltaic generator, a step-up converter connected in parallel with a DC side capacitor, a three-phase four-wire shunt active power filter based on voltage source inverter, and connected to the network in parallel with three nonlinear loads.

The effectiveness of the proposed PVG-SAPF counted on the method used for extracting the reference currents and the switching pulses generation. In this work, SRF theory [18-20] is used under unbalanced nonlinear load.

3.1. Synchronous Reference Frame (SRF) Theory

Synchronous reference frame theory is used first for three-phase three-wire active power filter (APF) and gave good results. Then this theory is generalized for three-phase four-wire APF based on the modification of the cross-vector theory of dqo-axes [21, 22]. The three-phase instantaneous nonlinear load currents (i_{La}, i_{Lb} and i_{Lc}) are modified from the (*a-b-c*) coordination into (*α-β-0*) coordination as follows:

$$\begin{bmatrix} i_\alpha \\ i_\beta \\ i_0 \end{bmatrix} = \sqrt{\frac{2}{3}} \begin{bmatrix} 1 & -\frac{1}{2} & -\frac{1}{2} \\ 0 & \frac{\sqrt{3}}{2} & -\frac{\sqrt{3}}{2} \\ \frac{1}{\sqrt{2}} & \frac{1}{\sqrt{2}} & -\frac{1}{\sqrt{2}} \end{bmatrix} \begin{bmatrix} i_{La} \\ i_{Lb} \\ i_{Lc} \end{bmatrix} \quad (3)$$

In this theory, the PLL (phase locked loop) is used to generate *cos (θ)* and *sin (θ)* from the three-phase source voltage v_{sa}, v_{sb} and v_{sc}. Then the cross-vector theory gives:

$$\begin{bmatrix} i_d \\ i_q \\ i_{q_\alpha} \\ i_{q\beta} \end{bmatrix} = \begin{bmatrix} 0 & \sin(\theta) & -\cos(\theta) \\ 0 & \cos(\theta) & \sin(\theta) \\ -\cos(\theta) & 0 & 0 \\ -\sin(\theta) & 0 & 0 \end{bmatrix} \begin{bmatrix} i_0 \\ i_\alpha \\ i_\beta \end{bmatrix} \quad (4)$$

The i_d and i_q currents include DC and AC values corresponding to the fundamental and harmonic currents respectively;

$$\begin{bmatrix} i_d \\ i_q \end{bmatrix} = \begin{bmatrix} \bar{i}_d & \tilde{i}_d \\ \bar{i}_q & \tilde{i}_q \end{bmatrix} \quad (5)$$

The DC part of i_d currents is taken out using a low pass filter. Then the currents in *α–β–0* by the following equation:

$$\begin{bmatrix} i_{0\_ref} \\ i_{\alpha\_ref} \\ i_{\beta\_ref} \end{bmatrix} = \begin{bmatrix} 0 & 0 & -\cos(\theta) & -\sin(\theta) \\ \sin(\theta) & \cos(\theta) & 0 & 0 \\ -\cos(\theta) & \sin(\theta) & 0 & 0 \end{bmatrix} \begin{bmatrix} \tilde{i}_d \\ i_q \\ i_{q\alpha} \\ i_{q\beta} \end{bmatrix} \quad (6)$$

The estimated current in the coordination a-b-c can be calculated as follows:

$$\begin{bmatrix} i_{fa\_ref} \\ i_{fb\_ref} \\ i_{fc\_ref} \end{bmatrix} = \sqrt{\frac{2}{3}} \begin{bmatrix} 1 & 0 & \frac{1}{\sqrt{2}} \\ -\frac{1}{2} & \frac{\sqrt{3}}{2} & \frac{1}{\sqrt{2}} \\ -\frac{1}{2} & -\frac{\sqrt{3}}{2} & \frac{1}{\sqrt{2}} \end{bmatrix} \begin{bmatrix} i_{0\_ref} \\ i_{\alpha\_ref} \\ i_{\beta\_ref} \end{bmatrix} \quad (7)$$

The reference currents are compared with their actual compensating currents in a hysteresis controller to generate the required switching pulses for the SAPF. Figure 7 shows the SRF theory Simulink diagram.

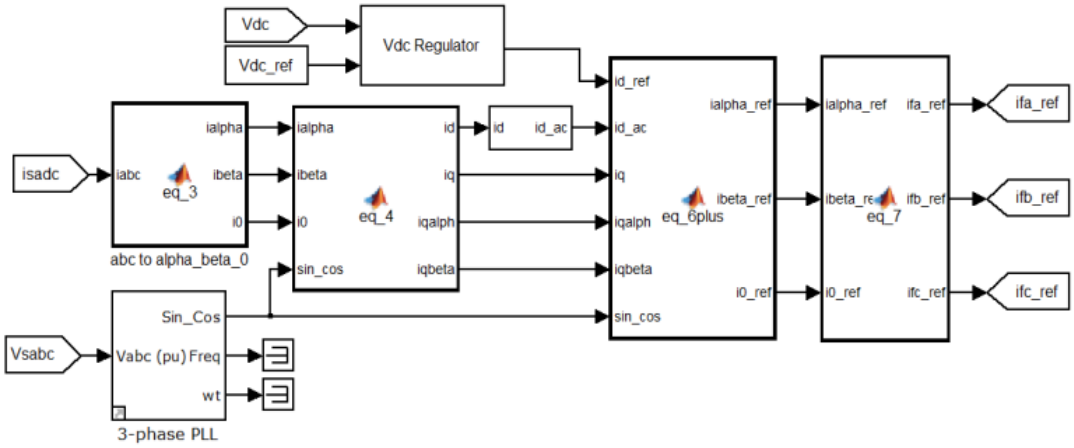

Figure 7. SRF Theory under Matlab/Simulink

4. Simulation Results and Discussion

Figure 8 shows the design of the developed PVG-SAPF under Matlab/Simulink software environment. The characteristics of the proposed system are given in table 2. The PV generator from CS5P-220M panel model consists of eight PV modules connected in series.

Table 2. PVG-SAPF System Characteristics

parameters		Values
Power supply	Voltage *rms, frequency*	*220 V, 50 Hz*
	Line mpedan-ce *(R_s, L_s)*	*0.5 mΩ, 0.19 µH*
SAPF	Inductance L_f	*0.32 mH*
DC capacitor	Capacitor C_{dc}	*4 mF*
DC voltage	*Vdc*	*750 V*
	Load1 *(R_l, L_l)*	*6 Ω, 0.012 H*
Unbalanced Nonlinear load	Load2 *(R_2,L_2)*	*4.5 Ω, 0.09 H*
	Load3 *(R_3,L_3)*	*3.6 Ω, 0.01 H*

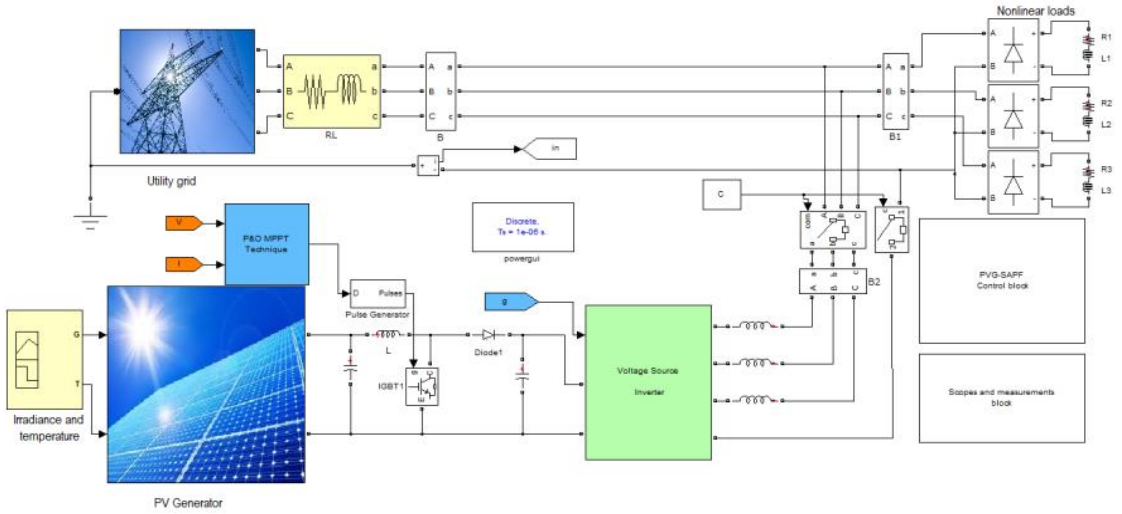

Figure 8. Matlab/Simulink based simulation of the designed PVG-SAPF

Figure 9(a) shows the different variations of irradiance, the MPPT based on P&O method follows quickly the prospective maximum power point in a brief time, and it works to regulate the duty cycle rapidly as presented in Figure 9(b). The P&O MPPT algorithm is robust against fast variation in atmospheric conditions, with few oscillations around MPP, and with high efficiency (up to 92%). The output voltage of the PVG is shown in Figure 10(a), while the dc-bus voltage (Vdc) and its reference voltage (Vdc_ref) are shown in Figure 10.b shows. The results prove that the system works well because the dc-bus voltage follows the reference voltage signal under variable irradiance.

The simulation results for the PVG-SAPF performing the current compensation and considering the three loads presented in Table 2 are illustrated in Figures 11-16. Without PVG-SAPF, the three nonlinear loads absorb non-sinusoidal currents, the source currents are deformed, unbalanced, and they are not in phase with their voltages as shown in Figure 11(a). With PVG-SAPF, which can supply the solar energy from the PV generator into the network, it injects at the point of common coupling (PCC) a current that is similar to the reference current (ifabc _ref, Figure 12(a)), but with a phase shift of 180° as shown in Figure 11(b). The observation of the PVG-SAPF tracking of injected currents ifabc and reference currents iref_abc is made with nearly zero error for the SRF theory as shown in Figure 12.b. The PVG-SAPF has enforced waveform sinusoidal source currents as displayed in Figure 11(c); in addition, the source currents are balanced.

Moreover, the obtained current and the source voltage are in phase as illustrated in Figure 12(c). Without PVG-SAPF, the form of the neutral current has a maximum value 55 A as shown in Figure 13(a). With PVG-SAPF, the source neutral current is approximately equal to zero as shown in Figure 13(b). Figure 14-16 show the FFT analysis of three-phase source currents (isa, isb, isc) without PVG-SAPF and with PVG-SAPF. The THD's are given in Table 3. It can be observed that these THD's values without PVG-SAPF are very high and unacceptable. The THD's are reduced with PVG-SAPF and SRF theory gives very good results under unbalanced nonlinear loads. The different results affirm the high quality of harmonic mitigation after using the proposed PVG-SAPF, a flawless compensation of reactive power and the reduction of the neutral current magnitude are observed.

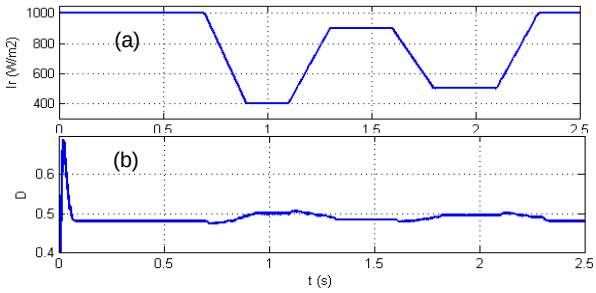

Figure 9. (a) Variation of Irradiance Ir (W/m2) and (b) duty cycle (D)

Table 3. THD (%) values after and before filtering

Phases	THD% before filtering	THD after filtering
Phase a	21.11%	2.98%.
Phase b	24.46%	2.67%
Phase c	29.97%	2.50%

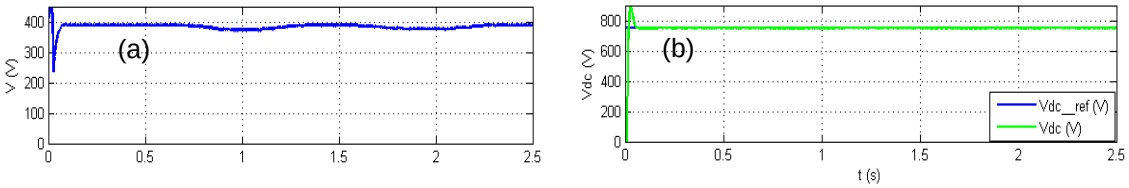

Figure 10. (a) PVG voltage V (V),(b) dc-bus voltage (Vdc(V)) and voltage reference (Vdc_ref (V)) under varying irradiance

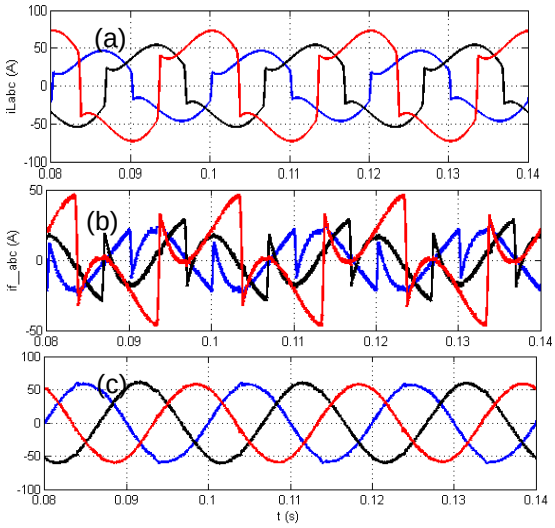

Figure 11. (a) Source currents without PVG-SAPF, (b) PVG-SAPF injected currents and (c) source currents with PVG-SAPF

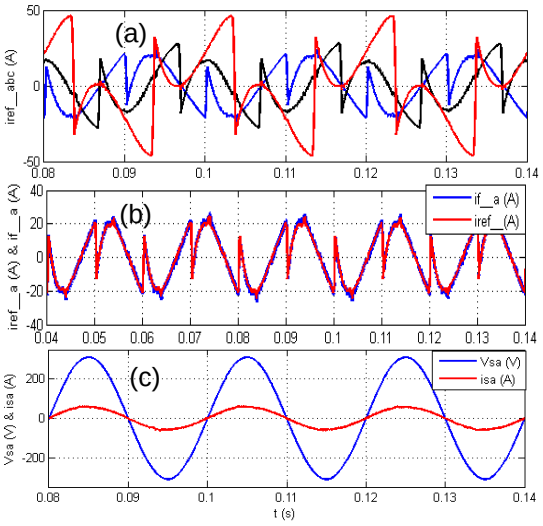

Figure 12. (a) Reference currents, (b) reference and injected currents and (c) power factor correction with PVG-SAPF (phase-a)

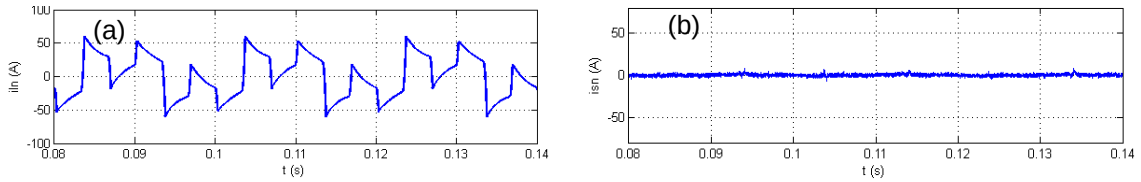

Figure 12. Neutral source current (a) without PVG-SAPF and (b) with PVG-SAPF

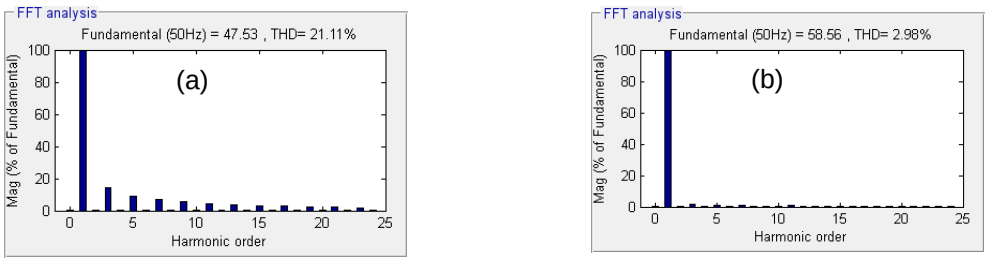

Figure 13. FFT analysis of source current (i_{sa} (A)): (a) without PVG-SAPF, (b) with PVG-SAPF

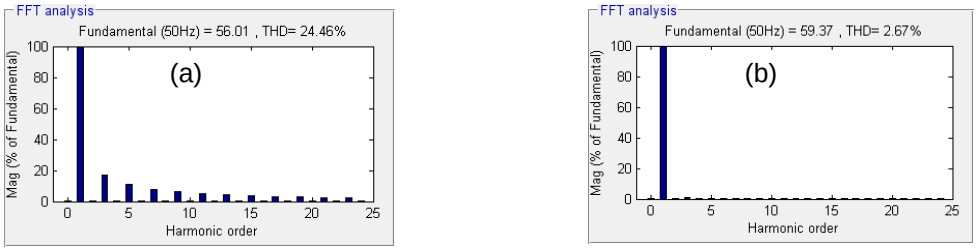

Figure 14. FFT analysis of source current (i_{sb} (A)): (a) without PVG-SAPF, (b) with PVG-SAPF

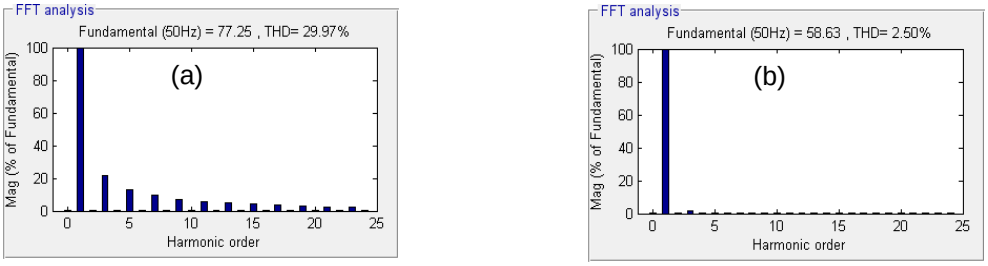

Figure 15. FFT analysis of source current (i_{sc} (A)): (a) without PVG-SAPF, (b) with PVG-SAPF

5. Conclusion

In this work, an association of GPV and a three-phase four-wire SAPF and PVG is proposed. The PVG-SAPF allows harmonics filtering, reactive power compensation for power factor correction, and load balancing, as well as injecting the issued energy from the PVG into the network. The SRF theory is used under unbalanced nonlinear loads. A PVG-SAPF consisting of voltage source inverter is employed. In order to increase the efficiency of maximum power point tracking, an MPPT control based on P&O is implemented in DC/DC converter. The simulation of the proposed system has been carried out using Matlab/Simulink software. The results demonstrate that the source currents have sinusoidal waveforms with very low THDs after using the proposed PVG-SAPF. In addition, the source voltage and their corresponding currents are in phase and well balanced, which performs the enhancement of the electrical power quality.

The obtained results confirm the high mitigation of harmonic currents, the flawless compensation of reactive power and the neutral current magnitude reduction for load balancing.

References

[1] Park TJ, Jeong GY, Kwon BH. Shunt active filter for reactive power compensation. *International Journal of Electronics*. 2001; 88: 1257-1269.

[2] Jain SK, Agarwal P, Gupta H. A Dedicated Microcontroller based Fuzzy Controlled Shunt Active Power Filter. *Intelligent Automation & Soft Computing*. 2005; 11: 33-46.

[3] Srikanth K, Mohan TK, Vishnuvardhan P. *Improvement of power quality for microgrid using fuzzy based UPQC controller*. Electrical, Electronics, Signals, Communication and Optimization (EESCO), 2015 International Conference on: IEEE. 2015: 1-6.

[4] Akagi H. Modern active filters and traditional passive filters. *Bulletin of the Polish Academy of sciences, Technical sciences*. 2006; 54.

[5] PitchaiVijaya K, Mahapatra K. Adaptive-fuzzy controller based shunt active filter for power line conditioners. *TELKOMNIKA (Telecommunication Computing Electronics and Control)*. 2013; 9: 203-210.

[6] Amirullah A, Penangsang O, Soeprijanto A. Power Quality Analysis of Integration Photovoltaic Generator to Three Phase Grid under Variable Solar Irradiance Level. *TELKOMNIKA (Telecommunication Computing Electronics and Control)*. 2016; 14: 29-38.

[7] Tali M, Obbadi A, Elfajri A, Errami Y. *Passive filter for harmonics mitigation in standalone PV system for non linear load*. 2014 International Renewable and Sustainable Energy Conference (IRSEC): IEEE. 2014: 499-504.

[8] Hong YY, Chiu CS, Huang SW. Multi-scenario passive filter planning in factory distribution system by using Markov model and probabilistic Sugeno fuzzy reasoning. *Applied Soft Computing*. 2016; 41: 352-361.

[9] Mahela OP, Shaik AG. Topological aspects of power quality improvement techniques: A comprehensive overview. *Renewable and Sustainable Energy Reviews*. 2016; 58: 1129-1142.

[10] Bendib B, Belmili H, Krim F. A survey of the most used MPPT methods: Conventional and advanced algorithms applied for photovoltaic systems. *Renewable and Sustainable Energy Reviews*. 2015; 45: 637-648.

[11] Libo W, Zhengming Z, Jianzheng L. A single-stage three-phase grid-connected photovoltaic system with modified MPPT method and reactive power compensation. *IEEE Transactions on Energy Conversion*. 2007; 22: 881-886.

[12] Alik R, Jusoh A, Sutikno T. A Review on Perturb and Observe Maximum Power Point Tracking in Photovoltaic System. *TELKOMNIKA (Telecommunication Computing Electronics and Control)*. 2015; 13: 745-751.

[13] Safari A, Mekhilef S. Simulation and hardware implementation of incremental conductance MPPT with direct control method using cuk converter. *IEEE Transactions on Industrial Electronics*. 2011; 58: 1154-1161.

[14] Rezk H, Eltamaly AM. A comprehensive comparison of different MPPT techniques for photovoltaic systems. *Solar Energy*. 2015; 112: 1-11.

[15] Salmi T, Bouzguenda M, Gastli A, Masmoudi A. Matlab/simulink based modeling of photovoltaic cell. *International Journal of Renewable Energy Research (IJRER)*. 2012; 2: 213-218.

[16] Boumaaraf H, Talha A, Bouhali O. A three-phase NPC grid-connected inverter for photovoltaic applications using neural network MPPT. *Renewable and Sustainable Energy Reviews*. 2015; 49: 1171-1179.

[17] Reisi AR, Moradi MH, Jamasb S. Classification and comparison of maximum power point tracking techniques for photovoltaic system: a review. *Renewable and Sustainable Energy Reviews*. 2013; 19: 433-443.

[18] Mahela OP, Shaik AG. Power quality improvement in distribution network using DSTATCOM with battery energy storage system. *International Journal of Electrical Power & Energy Systems*. 2016; 83: 229-240.

[19] Belaidi R, Fathi M, Larafi MM, Kaci GM, Haddouche A. *Power quality improvement based on shunt active power filter connected to a photovoltaic array*. 2015 3rd International Renewable and Sustainable Energy Conference (IRSEC): IEEE. 2015: 1-6.

[20] Sundaram E, Venugopal M. On design and implementation of three phase three level shunt active power filter for harmonic reduction using synchronous reference frame theory. *International Journal of Electrical Power & Energy Systems*. 2016; 81: 40-47.

[21] Benhabib M, Saadate S. New control approach for four-wire active power filter based on the use of synchronous reference frame. *Electric Power Systems Research*. 2005; 73: 353-362.

[22] Chebabhi A, Fellah M, Kessal A, Benkhoris M. Comparative study of reference currents and DC bus voltage control for Three-Phase Four-Wire Four-Leg SAPF to compensate harmonics and reactive power with 3D SVM. *ISA transactions*. 2015; 57: 360-372.